Characterization of (111)B and (211)B CdZnTe Substrates for HgCdTe Growth

R. Haakenaasen[1,2,4], O. Lauten[1,3], E. Selvig[1], K.O. Kongshaug[1], E.J. Røer[1,3] and R.W. Hansen[1]

1. FFI – Norwegian Defence Research Establishment, P.O. Box 25, NO-2027-Kjeller, Norway.
2. University Graduate Center at Kjeller (UNIK), P.O. Box 70, NO-2027 Kjeller, Norway.
3. Department of Physics, Norwegian University of Science and Technology, Høgskoleringen 5, NO-7491 Trondheim, Norway.
4. e-mail: randi.haakenaasen@ffi.no, ph: +47 63 80 73 09, fax: +47 63 80 72 12

ABSTRACT

We have studied state-of-the-art CdZnTe (211)B and (111)B substrates and compared them to each other and to substrates from an alternative vendor. The CdZnTe surface has been characterized both as-received and after growth preparation procedures using dark field optical microscopy, scanning electron microscopy, energy-dispersive x-ray spectroscopy, atomic force microscopy, Fourier transform infrared transmission spectroscopy, and secondary ion mass spectroscopy. From these measurements we have obtained densities of particles and morphological defects with size > 0.5 μm, densities of small particles/features with size ≤ 100 nm, and substrate/film interface impurities. The state-of-the-art substrates all have remains of silica grit polishing particles around the edges. The as-received (111)B substrates had very few particles or morphological defects on the surface, but a Br:methanol surface preparation etch exposed a large number of features with sizes ≤ 100 nm. Some of these were silica grit particles, but most of them were Te precipitates. The (111)B substrate from an alternative vendor had a lot of different particles, stains, and voids. It improved significantly after a fine-polishing procedure, but still had the surface with most defects after surface preparation. The state-of-the-art (211)B had the largest as-received density of small features, but after Br:methanol etching this density (of Te precipitates and silica grit particles) was the same as for the etched (111)B substrate. SIMS measurements showed that some of the polishing grit particles ended up on the top surface after surface preparation. Hydrofluoric acid can be used to etch away the silica particles.

Key words: CdZnTe substrate, HgCdTe, Te precipitates, defects, polishing, impurity contamination

Dette er en postprint-versjon/This is a postprint version.
DOI til publisert versjon/DOI to published version: 10.1007/s11664-019-07349-6

INTRODUCTION

The highest performance infrared focal plane arrays are fabricated on $Hg_{1-x}Cd_xTe$ layers that are grown on $Cd_{1-y}Zn_yTe$ substrates. With $y \approx 0.04$, the substrates are approximately lattice-matched to the $Hg_{1-x}Cd_xTe$ lattice constant for midwave infrared (MWIR) to long wave infrared (LWIR) band gap material. Using a substrate which matches both in crystal structure and lattice constant is a great advantage in the otherwise difficult growth of this material. The ~1.6 eV band gap of CdZnTe results in relatively high resistivity and allows backside illumination. Disadvantages of CdZnTe are i) difficulty in growth of high quality crystals, resulting in impurities and defects, limited sizes and high cost, and ii) difficulty in surface preparation, resulting in particles and morphological defects on the surface. Also, a different thermal expansion coefficient from that of the Si read-out integrated circuit necessitates removal of the substrate for larger arrays.

The quality of the HgCdTe layers grown on CdZnTe will depend on both growth conditions and on substrate quality (morphological defects, impurities, particles).We have earlier described defects in molecular beam epitaxy (MBE)-grown HgTe and HgCdTe layers.[1-3] The optimal growth temperature of HgCdTe is just below the Te phase limit.[4,5] With increasing deviation below this temperature, there will be an increasing number of microvoids, while a higher temperature will result in more and larger high temperature voids (also called voids in the literature). We have suggested that the microvoids are formed by a preferential surface diffusion of the Te atoms in the [111] direction on (211)B substrates, whereas on a symmetric plane, such as (111)B, they have no preferential diffusion direction. If a particle/impurity on the surface is blocking the diffusion of Te atoms, the result will be a build-up of material on the upstream (step-flow-direction) side of the impurity. On the downstream side of the impurity there will be a deficiency of material, i.e. a void. This is in agreement with the topography and composition of the microvoids.[1-3] We found that particles/dust on the substrate surface could give rise to microvoids. The high temperature voids, which are Hg-poor and Te-rich, may be associated with Te precipitates in the substrate.[6] They can get very large and destroy detector diodes.

Benson et al. have studied (211)B substrates from JX Nippon Mining & Metals Corporation, Japan (Nippon), which are generally considered state-of-the-art substrates for HgCdTe growth.[7-10] They found that the as-received substrates had a significant amount of impurity contamination, particles, Te precipitates and scratches on the surface, and they concluded the substrates were not epi-ready out of the box.

In this paper we describe a complementary study where we compare the as-received and after surface preparation (111)B substrates from Nippon (used in liquid phase epitaxy (LPE) growth of HgCdTe), (111)B substrates from an alternative source, and (211)B substrates (used in MBE growth of HgCdTe) from Nippon.[11]

Dette er en postprint-versjon/This is a postprint version.
DOI til publisert versjon/DOI to published version: 10.1007/s11664-019-07349-6

We have used optical microscopy, scanning electron microscopy (SEM) with energy dispersive x-ray spectroscopy (EDS), atomic force microscopy (AFM), Fourier-transform infrared spectroscopy (FTIR) and secondary ion mass spectroscopy (SIMS). The as-received substrates were characterized, then polishing and/or etching processes were performed on the substrates, and they were characterized a second time. We found that the number of particles and defects on the as-received and etched (211)B substrates were large and agreed with the numbers found by Benson et al.[8,9] However, our interpretation of these features is different. Furthermore, the (111)B substrates gave the surprising result that there were very few features on the as-received substrate, but after the growth preparation etch the density of morphological defects/features on the surface increased considerably. Our polishing process improved the surface of the alternative substrates substantially, but they still were inferior to the surfaces of the Nippon substrates.

EXPERIMENTAL DETAILS

Three different types of CdZnTe substrates were analyzed. Substrates A and E (SubA and SubE) were 30 × 30 mm^2 (111)B substrates from Nippon, substrates B and B2 (SubB and SubB2) were 30 × 30 mm^2 (111)B substrates from an alternative vendor, and Substrates C and D (SubC and SubD) were 15 × 15 mm^2 and 25 × 25 mm^2 (211)B substrates from Nippon. In addition, some older 10 × 10 mm^2 (111)B substrates from Nippon were used in etching experiments. The growth side of all the substrates wase the Te-terminated B-face, and all images presented in the paper are from the B-face.

First the substrates were studied as-received. An overview of the substrate was obtained with bright field and dark field optical microscopy in a Leica DM RXA2 optical microscope, and a density of larger particles/morphological defects with size > 0.5 μm was measured. FTIR transmission spectra mapping was done by mounting the substrate in a home-made sample holder with two stepper motors run by a Testpoint program, all placed in a Perkin Elmer Spectrum GX FTIR . The substrates were mounted with a thin stripe of carbon tape on a SEM sample holder and loaded into a Hitachi SU6600-VP FEGSEM with a Bruker XFlash5010 detector for the EDS. A number of particles/morphological features were found and identified, and their surface densities were calculated when possible. High resolution images were taken with 2-5 kV accelerating voltage, while the EDS spectra were taken using 10 kV to ensure an electron energy larger than the peaks of interest, but still limited in order to maintain reasonable resolution.

The SEM sample holder was then attached to the magnetic sample holder of a PSIA AFM Park Systems XE-100 atomic force microscope, and AFM images were recorded in non-contact mode using a Nanosensors

Dette er en postprint-versjon/This is a postprint version.
DOI til publisert versjon/DOI to published version: 10.1007/s11664-019-07349-6

PPP-NCHR probe with aluminum coating on the detector side. The images were obtained using a scan rate of 0.2 Hz and a scan size of 5 µm, and particles, surface roughness and scratches were characterized.

Next, the substrates were treated with different surface preparations. As-received SubA and SubE were etched in a Br:methanol solution to remove ~ 2 µm. SubB had only been coarsely polished by the vendor, so we applied a fine-polishing process. This process involved using an alumina-based polishing slurry, and ~100 µm of material was removed. Subsequently SubB was etched in a Br:methanol solution in the same way as SubA and SubE, to remove ~ 2 µm. Unfortunately, SubB broke into pieces during the second round of characterization after polishing/etching. A second substrate from the alternative vendor (SubB2) was then polished and etched in the same way as SubB. SubB2 was only characterized after surface preparation. SubC and SubD were characterized as–received, cleaned with cold acetone and methanol, and then etched in a Br:methanol solution which removed ~ 4 - 5 µm.

.

RESULTS AND DISCUSSION

Beveled Edge – Nippon Substrates

All the substrates from Nippon had beveled edges on the B-face. A SEM image of a corner of SubE is shown in Fig. 1a, where we see the beveled edges, while Figs. 1b and 1c are higher magnification images from the edge itself. The outer, lighter-colored bands on the edge are dense layers of small, round particles approx. 50 – 100 nm in diameter, while the darker band closer to the plane surface has a lower concentration of the same particles in an area which is very uneven.

An EDS spectrum from the plane top surface of the substrate (away from the beveled edge) is plotted (grey) together with a spectrum from the beveled edge (black line) in Fig. 1d. The surface of the substrate consists of mainly Te, Cd and Zn, with concentrations 49.3/47.4/2.3 at.%, which is close to the nominal values of 50/48/2 at.%. There seem to be small peaks at the position of Si and Al, but we believe these are not from the sample as they appear in all spectra, also from as-grown samples. They are most likely due to Si in the dead layer of the Si detector and scattering of electrons from aluminum parts in the chamber or sample holder. On the bevel edge, however, we get large Si and O peaks of 15.1 at.% and 41.9 at.%, respectively, in addition to CdZnTe. The particles seen on the bevel edges are therefore believed to be SiO_2 (silica) grit particles left on the substrate after polishing/etching by the vendor. This agrees with the description of the substrate preparation by Nippon.[11] A small amount of chlorine detected may stem from NaClO commonly used as a cleaning agent after polishing.

Dette er en postprint-versjon/This is a postprint version.
DOI til publisert versjon/DOI to published version: 10.1007/s11664-019-07349-6

Relevant questions are whether there are also grit particles on the plane surface and if they disappear after a standard preparation etch. We will address these issues below.

Substrate A – 30 × 30 mm^2 (111)B CdZnTe from Nippon, as-Received

Fig. 2a shows a dark field image of as-received SubA. There were very few particles or other features to be seen; the density of morphological defects/particles/features with size > 0.5 μm (i.e. the larger features, n_L) was $n_L = 400$ cm^{-2}. This result was supported by a SEM investigation, in which we saw almost no features except for a few particles close to the bevel edges – as seen in Figs. 2b and 2c. The spectrum and the round shape of the 50-100 nm size particles in Fig. 2d points to alumina Al_2O_3 (alumina) and silica polishing grit, while the larger particle in Fig. 2e with size > 5 μm had the same EDS spectrum as the underlying substrate and was therefore believed to be CdZnTe debris from the cutting and polishing of the substrate. The rest of the top surface looked completely featureless, and it was therefore difficult to determine a particle 'density' on this as-received substrate. These results seem to be consistent with the descriptions of Noda et *al*., which state that Nippon uses alumina powders in lapping, colloidal silica in polishing, and a unique chemical final polishing solution.[11]

The AFM was used to study surface topography. A typical AFM image from the middle of the substrate is shown in Fig. 2f. Again, there were no particles or bumps/indentations seen on the surface. The root mean square (RMS) roughness was measured to be ~0.3 nm, which indicates the absence of large scratches. The typical surface scratches were 10 – 20 nm wide and 1 nm deep, while the largest were 200 nm wide and 5 nm deep. FTIR transmission spectra were recorded from an 11 × 11 grid on the as-received SubA. The grid points were placed 2.0 mm from the edge and had 2.6 mm between nearest neighbors. The curves are flat, and all but four measurements had an IR transmittance between 62 % and 67 % in the wavenumber range 1000 to 5000 cm^{-1}, as seen in Fig. 3a. The spikes near $k = 4500$ cm^{-1} and $k = 5000$ cm^{-1} were artefacts of the FTIR instrument and should be ignored. There is no significant free carrier absorption and the transmission level is good.[12,13] It has been shown that transmission levels are decreased by Te precipitates/inclusions, and higher transmission levels can be achieved in precipitate-free substrates.[14-16]

A map of the transmission at $k = 500$ cm^{-1} can be seen in Fig. 3b. The three slightly descending spectra are possibly due to surface roughness.[17] When combined with the extremely low particle density, it does indeed seem that the quality of this substrate, as-received, is very good. The densities of particles and AFM roughness before and after surface preparation are listed in Table I.

Dette er en postprint-versjon/This is a postprint version.
DOI til publisert versjon/DOI to published version: 10.1007/s11664-019-07349-6

Substrate A – after surface preparation etching

To prepare SubA for LPE growth of HgCdTe, it was etched in a Br:methanol solution. The density of large particles/features increased somewhat to $n_L = 1\times10^3$ cm^{-2}. A dark field image is shown in Fig. 4a, a typical SEM image from the middle of the substrate is shown in Fig. 4b, some of the larger particles/stains close to the bevel edges in Fig. 4c, an AFM image from the middle of the substrate in Fig. 4d, and in Fig. 4e the EDS spectrum from an area similar to that in Fig. 4b. The particles in Fig. 4c were 0.5-20 μm 'flakes' of silica grit particles (upper) and 10-20 μm stains/particles (lower) which contained bromine, carbon and oxygen in their spectra. The flakes must come from the grit layers on the beveled edges, as we did not use silica grit on these substrates.

The big surprise here, however, was the dramatic increase in the density of small particles/features, n_S, on the surface, from practically none to ranging from $n_S = 2\times10^5 - 1\times10^7$ cm^{-2} with an average $n_S = 2\times10^6$ cm^{-2}, as illustrated in the SEM image in Fig. 4b. These small ≤ 100 nm features were all over the surface. We also clearly see particles in the AFM images, with size 10-50 nm and height 10 nm above the surface, such as in Fig. 4d.

What are these small particles or features? It was first believed that they were silica grit particles coming from the bevel edges. However, the EDS spectrum of the etched surface in Fig. 4e looks the same as before etching. There is not enough Si and O for so many grit particles. Furthermore, the AFM height is not consistent with 50-100 nm spherical particles.

We then looked at images of backscattered electrons (BSE) in the SEM, where the contrast in composition mode comes from atomic number which is reflected in the mass density. An example is shown in Fig. 5a, where a lump of 4 white grit particles in the secondary electron (SE) image are dark in the corresponding BSE image. This is as expected, as silica has much lower average Z than CdZnTe. But there are also a lot of smaller particles that have lighter color than the matrix in the BSE image and thus cannot be grit nor CdZnTe. Fig. 5b shows SE and BSE images of one grit particle and one 'other' feature. Generally, the grit particles are round in shape, with a very well defined border/edge and with a lot of Si and O in their EDS spectra. The other small particles are of varying shape and size, and with fuzzy rather than well-defines edges. From the bright middle they seem to fade away into the matrix. It is difficult to see the difference between the EDS spectra from the particles and from the matrix. We believe, however, that these particles must be Te precipitates/inclusions, which is consistent with them being a little heavier than CdZnTe, having varying shapes, and the fact that they fade away into the matrix background. They stand out 10 nm above the surface, according to the AFM measurements. As they are so small, a very small additional Te signal, on top of the Cd, Zn and Te signals from the matrix, is hardly visible in

Dette er en postprint-versjon/This is a postprint version.
DOI til publisert versjon/DOI to published version: 10.1007/s11664-019-07349-6

EDS. There are silica grit particles on the surface as well, but these make up less than 10 % of the small features (and thereby of n_S).

The Te precipitates appear in all sizes from very small (~20 nm) up to at least 5 μm. Figs. 6a and 6b show SE and BSE images of a 'pattern' of very small Te precipitates, but in Fig. 6b there is a large Te precipitate in the middle. Perhaps the slightly higher concentration of Te in the pattern in Fig. 6a is the beginning of the formation of the larger Te precipitate in Fig. 6b. The EDS spectrum from a big precipitate, similar to the one in Fig. 6b, is shown in Fig. 6c (black line) along with a spectrum from the surface away from the precipitate (blue). The actual precipitate is shown in the inset. Here we got a large Te signal and found that the area had 78 at.% Te, 11 at.% Cd and 11 at.% C.

The RMS roughness was measured by AFM to be 0.51 nm in the center of SubA, an increase by almost a factor 2, which was mainly due to the particles. Close to the edges the roughness was 1.3 nm, and the surface looked grainier. EDS analysis of a large area of the surface gave the same composition as before etching.

Thus, SubA as-received had an extremely smooth surface with almost no particles or morphological features, while the Br:methanol etch seemed to expose Te precipitates of all sizes up to many microns. The precipitates can be underneath CdZnTe, exposed, or released and in some cases stuck somewhere else on the surface. In Fig. 7a a small piece of a diamond-shaped Te precipitate seems to have broken off and re-attached a little distance away. The Br:methanol etch did not directly etch/dissolve silica grit particles, but it etched the CdZnTe on the beveled edges, thereby releasing flakes of silica grit, some of which got attached close to the edges. There was little grit in the middle of the substrate. SubE was similar to SubA and was used to back up the results from SubA.

Substrates B and B2 – 30 × 30 mm^2 (111)B CdZnTe from an Alternative Source, as-Received

We wanted to study a substrate from an alternative source, both to compare the substrate quality and to check our surface fine-polishing technique. SubB had only been roughly polished by the vendor. A typical dark field image of the surface is shown in Fig. 8a. It is very different from the as-received SubA in Fig. 4a. Polishing scratches in all directions and with varying width, particles and morphological defects with both small (0.5 - 5 μm) and large (5 - 50 μm) diameter were present on the surface. From the dark field image, the density of larger particles and morphological defects was estimated to be $n_L = 1\times10^5$ cm^{-2} on the surface. SEM images show both bright spots and dark stains on the surface, Fig. 8b, and a density of small particles/features $n_S = 6\times10^5$ cm^{-2}.

Dette er en postprint-versjon/This is a postprint version.
DOI til publisert versjon/DOI to published version: 10.1007/s11664-019-07349-6

Scratches were seen with SEM and characterized with AFM, Fig. 8c. The RMS roughness was 4 nm, which is 16 times larger than on as-received SubA. The largest polishing scratches were 300 nm wide and 15 nm deep. The following particles/features were found with SEM/EDS on the surface, some of which are shown in Fig. 9: (a) alumina and silica grit particles, (b) CdZnTe, (c) dark particles with size 20-30 µm containing a lot of carbon (could be residue from mounting wax), (d) and (e) a stained area had particles with Na, Cl and O which could be NaClO from cleaning solution that is typically used to remove polishing slurry particles, (f) an iron particle which could be a contaminate in polishing slurry, (g) circular bright stains, (h) dark stains and (i) and (j) voids of size 5-100 µm all over the surface.

The voids had the same composition as the matrix, and AFM measured them to be 5 - 100 µm wide and 1-3 µm deep. The void density varied from 2×10^3 cm^{-2} – 2×10^4 cm^{-2}, with average of 7×10^3 cm^{-2}, over the surface. Some of the smaller voids had a threefold symmetry, as seen in Fig. 9j. The larger voids (> 10 µm) tended to have multiple angular features. Circular stains, Fig. 9g, had size 30-150 µm with density 2×10^2 cm^{-2}, and could be residue from the evaporation of a droplet on the surface, with the center consisting of the impurities that were carried by the surface tension of the droplet. These look similar to stains described by Benson et *al.*[10]

FTIR transmission spectra and a map of the transmission in SubB2 at 500 cm^{-1} are shown in Figs. 10a and 10b. There is absorption in all the spectra, but much more so in the lower half of the substrate, where an area of very low transmission forms a semicircle. The shape of these spectra are characteristic of free carrier absorption due to holes.[12,13] As we have not found high concentrations of acceptor impurities in these substrates, we believe the holes are due to Cd vacancies.

Substrates B and B2 – after surface preparation polishing and etching

SubB and SubB2 were fine-polished and etched as described above. This improved the surface considerably. The dark field images had fewer bright spots, the previously observed deep surface scratches were removed, and there were far less particles and other features on the substrate surface, as seen in Fig. 11a. The large particle density had decreased by a factor 20 to $n_L = 5\times10^3$ cm^{-2} on SubB and the same density was measured on SubB2. Typical SEM images from the center of the two substrates are shown in Figs. 11b and 11c. The small-particle density had increased by approximately a factor 17 to $n_S = 7\times10^6$ cm^{-2} on SubB, whereas it was measured to $n_S = 1\times10^7$ cm^{-2} on SubB2. Only four types of particles were now observed beside the Te

Dette er en postprint-versjon/This is a postprint version.
DOI til publisert versjon/DOI to published version: 10.1007/s11664-019-07349-6

precipitates: alumina grit particles and agglomerations of these, Fig. 11d, 5-50 μm long CdZnTe particles, HgTe particles, Fig. 11e, and some particles consisting of F and C, in a ratio consistent with C_2F_5, Fig. 11f. The alumina grit was remains from our own polishing process, while the origin of the HgTe may be impurities in our lab and the presence of the C-F particles is a mystery. The AFM RMS roughness near the center was 0.88 nm/0.91 nm for SubB/SubB2, which for SubB was a decrease to ¼ that of the as-received, Fig. 11g. The surface scratches had been removed. EDS of the center of SubB gave the same CdZnTe composition as before the polish.

Our fine-polish process clearly is not as good as the one from Nippon: while their SubA as-received had almost no particles on the surface, our polished and etched SubB and SubB2 had a high density of small particles (n_S). It will be better to compare the etched SubA with polished and etched SubB/SubB2. The Te precipitate density was a factor 3.5 - 5 larger on SubB/B2 than on SubA after Br:methanol etch. The surface roughness was almost twice as large on B/B2. Finally, half of SubB had a lower IR transmission. SIMS samples were prepared from an LPE HgCdTe layer grown on a similar substrate with varying transmission. The SIMS profiles are presented below.

Substrate C – 15 × 15 and 25 × 25 mm^2 (211)B CdZnTe from Nippon, as-Received

The as-received 15 ×15 mm^2 (211)B SubC had a small number of dark field features of size 1-15 μm close to the edges ($n_L = 3 \cdot 10^1$ cm^{-2}), as seen in Fig. 12a, which is not very different from SubA. However, the SEM images revealed a large number of particles/morphological features of size 20-100 nm scattered all over the surface, see Fig. 12b. This is in contrast to as-received SubA – also from Nippon, but (111)B oriented - which had basically no features to be seen in the SEM (Fig. 2b). Although some of the features on SubC were single or agglomerations of silica grit particles, the majority were again consistent with Te precipitates. The density of Te precipitates varied from $n_S = 1{\times}10^6 – 5{\times}10^7$ cm^{-2}. The average was counted in 24 SEM images to be $n_S = 3{\times}10^7$ cm^{-2}, which is larger than on any of the other substrates in this study, etched or not. In total, particles on 0.005% of the surface area were counted. The number density here was in agreement with that of Benson et al. for (211)B Nippon substrates, but while they found the particles to be silica grit before etching and CdZnTe after Br:methanol etching, we believe they are largely Te precipitates.[8,9] In our study, silica grit particles were mostly found close to the beveled edges, but had a low density. A small agglomeration of such grit particles is shown in Fig. 12b. A few large carbon-based particles were also observed on the surface. They could be residue from mounting wax used during polishing by the vendor.

Dette er en postprint-versjon/This is a postprint version.
DOI til publisert versjon/DOI to published version: 10.1007/s11664-019-07349-6

AFM images of smaller areas gave a particle density $n_S = 6\times10^7$ cm^{-2} for particles with size 50-200 nm and height 10 nm, such as seen in Fig. 12c. This supports the classification of the particles being Te precipitates in the substrate and not round 50 nm particles on top of the surface. AFM scans revealed a surface RMS roughness at the center of SubC of 0.3/0.95 nm for surface without/with Te precipitates. The small value indicates an absence of deep scratches. The deepest observed scratch was 0.2 µm wide and 1 nm deep. Benson et al. measured an RMS roughness of 0.4 nm on as-received (211)B substrates.[8]

FTIR transmission spectra were recorded from a 5 × 5 grid on the as-received SubC. The transmission spectra and a transmission map at 500 cm^{-1} are shown in Fig. 13. All but five spectra had the same characteristics as spectra from SubA, see Fig. 3a. The five spectra from the upper edge of the sample had the same shape as the rest of the spectra, but with the transmission lowered by the same amount at all wavenumbers. We believe this is simply because the frame that holds the sample blocks some of the light at the top.

Substrate C – After Surface Preparation Etching

SubC was etched in Br:methanol as described above (slightly different from the LPE growth preparation etch) and 4 - 5 µm of material was removed. A dark field image is shown in Fig. 14a. The dark field density of larger particles/features had increased and was $n_L = 8\times10^3$ cm^{-2} at the center. A SEM image near the center of the substrate with inserts of silica grit, a flake of silica grit and a carbon particle are shown in Fig. 14b. An AFM image is shown in Fig. 14c.

The density of small particles n_S (Te precipitates + silica grit particles) had decreased by almost a factor of 10 to $n_S = 3\times10^6$ cm^{-2} and was now close to the n_S of etched SubA. Four types of particles were seen in addition to the Te precipitates: silica grit particles and large flakes of these close to the edges (Fig. 14b), particles with C, Br, N and S, and other particles with C, Br and O in their spectra. The surface roughness was found to be 1.4 nm at the center, which was a 50% increase from before etching.

It seems that the vendor uses different processes on the (211)B and the (111)B substrates. Perhaps this has to do with what the substrates are used for. The (211)B substrates have to be cut at a 19.5° angle with the (111)B plane, and the surface then consists of closely spaced (111)B terraces. After the beveled edge has been formed, silica grit is used to polish the sample surface, and on (211)B that is probably followed by a Br:methanol etch. Then another Br:methanol etch is performed before loading the sample into the MBE machine. Whatever is on the surface going into the growth chamber, stays on the surface/interface and gets incorporated into the grown

Dette er en postprint-versjon/This is a postprint version.
DOI til publisert versjon/DOI to published version: 10.1007/s11664-019-07349-6

film. It could be that the unique chemical final polishing solution leaves unwanted impurities (for example Cl) on the surface and therefore can't be used on the MBE substrates.

The beginning of the LPE growth process is different: the melt is so hot that a thin layer of the (111)B substrate surface is actually dissolved into the melt. This may make the LPE process less sensitive to some impurities on the surface, depending on how fast the impurities get incorporated into the growing film.

We have tried several procedures to remove the bevel grit layers. The only thing that worked was etching in hydrofluoric acid (HF); this dissolves the silica particles. HF removes oxides, whereas Br:methanol seems to expose Te precipitates. It would be interesting to just do an HF etch as the growth preparation procedure.

SIMS profiles

We sent samples of HgCdTe films, grown on similar substrates to the ones described above, to Evans Analytical Group (EAG) for SIMS profiling, These were: an MBE-grown film ($x = 0.29$) on a (211)B Nippon substrate, an LPE-grown film ($x = 0.23$) on a (111)B Nippon substrate, and two samples from areas with different transmission levels (high and low transmission) from the same LPE-grown film ($x = 0.23$) on a (111)B alternative substrate.

Some of the profiles from the four samples are shown in Fig. 15, and there are labels with arrows to the peaks on the top of the graph. The interface depths are at approximately 13, 19, 21 and 28 μm, for the four samples. The peaks in the Si profiles on the substrate/film interface are significantly larger in the Nippon substrates than in the two samples from the alternative substrate, Fig. 15a. In Fig. 15b it is opposite – there is more Al on the interface in the samples from the alternative substrate. This makes sense as we used alumina grit to polish the alternative substrates. No silica grit was used in our lab on these substrates, so the grit particles on the Nippon surfaces and interfaces must come from the silica grit used by Nippon. So it does indeed seem that some of the silica grit gets into the HgCdTe films. Also interesting is the shape of the peaks: in the MBE-grown sample the peaks are narrow because what is on the surface going into the growth chamber, stays on the surface, and is covered by HgCdTe. In the LPE samples, the peaks are broader, especially for Si. This may be because remaining silica grit from the beveled edges also become part of the initial melt. When re-depositing on the growing surface, it contributes to a higher density of silica grit on the top surface than before growth.

Another interesting profile is that of Fe. In the LPE-grown films it has a broad peak with full width half maximum (FWHM) of 3.4 μm, while the Al and Si peaks at the substrate/HgCdTe interface have FWHM = 0.2 μm. The Fe peak is almost equal in the LPE-on-Nippon and the high transmission sample from LPE-on-

Dette er en postprint-versjon/This is a postprint version.
DOI til publisert versjon/DOI to published version: 10.1007/s11664-019-07349-6

alternative-substrate, while it is ~ 3.6 times larger in the low transmission sample from LPE-on-alternative-substrate. Still, it is not very large, and it remains a question whether it has something to do with the lower transmission. In the MBE-grown sample the Fe peak is much narrower (FWHM = 0.12 μm).

CONCLUSIONS

Among the substrates in the study, the best one was the as-received (111)B SubA from Nippon. It had hardly any particles or morphological defects on the surface, even though it did have an almost continuous layer of silica grit particles on the beveled edges around the perimeter of the substrate. A Br:methanol etch exposed a lot of Te precipitates of all sizes that were probably distributed throughout the substrate volume. Br:methanol dissolves CdZnTe and thereby releases the layers of silica grit on the bevel edges by undercutting them. During this process, large (1-20 μm) flakes of silica grit can get stuck on the surface, but mostly near the edge it came from. However, there was enough silica grit, either on the surface or distributed in the LPE film during growth, that a SIMS profile through a HgCdTe film grown on a similar substrate showed a large Si peak at the film-substrate interface.

SubA was compared to (111)B SubB from an alternative vendor. SubB was only roughly polished and had deep scratches, many different particles, and higher surface roughness, than SubA. After polishing and Br:methanol etching, the number of particles on the surface had increased to the highest number for all the growth prepared substrates in this study. SIMS profiles of a HgCdTe film grown on a similar substrate showed a smaller Si but larger Al concentration at the film-substrate interface than in SubA. This is reasonable since SubA was polished with silica grit, and has remains of this on the beveled edges, while SubB was polished with alumina grit.

The (211)B as-received SubC from Nippon looked completely different from as-received SubA from the same vendor. It had the highest as–received density of small particles $n_S = 3\times10^7$ cm^{-2}, (size ≤ 100 nm), but this decreased by a factor 10 after the Br:methanol etch, to end up with the same density as the etched SubA at $n_S = 3\times10^6$ cm^{-2}. Most of these were Te precipitates, but there were also silica grit particles and agglomerations of these. It seems the vendor must use different processes to prepare these substrates - Br:methanol for (211)B and something else for (111)B substrates.

Dette er en postprint-versjon/This is a postprint version.
DOI til publisert versjon/DOI to published version: 10.1007/s11664-019-07349-6

A hydrofluoric acid etch dissolved silica particles but not CdZnTe. It has the potential to get rid of the silica grit while neither depositing grit on the surface nor increasing the surface roughness.

SIMS measurements showed that substrate areas with lower transmission had a larger Fe peak at the substrate-film interface than the areas with high transmission.

Dette er en postprint-versjon/This is a postprint version.
DOI til publisert versjon/DOI to published version: 10.1007/s11664-019-07349-6

REFERENCES

1. E. Selvig, C.R. Tonheim, K.O. Kongshaug, T. Skauli, T. Lorentzen and R. Haakenaasen, *J. Vac. Sci, Technol., B* 25, 1776 (2007).
2. E. Selvig, C.R. Tonheim, K.O. Kongshaug, T. Skauli, H. Hemmen, T. Lorentzen and R. Haakenaasen, *J. Vac. Sci, Technol., B* 26, 525 (2008).
3. E. Selvig, C.R. Tonheim, T. Lorentzen, K.O. Kongshaug, T. Skauli, and R. Haakenaasen, *J. Electron. Mater.* 37, 1444 (2008).
4. T. Colin and T. Skauli, *J. Electron. Mater.* 26, 688 (1997).
5. T. Colin, D. Minsås, S. Gjøen, R. Sizman and S. Løvold, *Mater. Res. Soc. Symp. Proc.* 340, 575 (1994)
6. Y. Chang, C.R. Becker, C.H. Grein, J. Zhao, C. Fulk, T. Casselman, R. Kiran, X.J. Wang, E. Robinson, S.Y. An, S. Mallick, S. Sivananthan, T. Aoki, C.Z, Wang, D.J. Smith, S. Velicu, J. Zhao, J. Crocco, Y. Chen, G. Brill, P.S. Wijewarnasuriya, N. Dhar, R. Sporken and V. Nathan, *J. Electron. Mater.* 37, 1171 (2008).
7. J.D. Benson, L.O. Bubulac, P.J. Smith, R.N.Jacobs, J.K. Markunas, M. Jaime-Vasquez, L.A. Almeida, A. Stoltz, P.S. Wijewarnasuriya, G. Brill, Y. Chen, J. Peterson, M. Reddy, M.F. Vilela, S.M. Johnson, D.D. Lofgreen, A. Yulius, G. Bostrup, M. Carmody, D. Lee and S. Couture, *J. Electron. Mater.* 43, 3993 (2014).
8. J.D. Benson, L.O. Bubulac, M. Jaime-Vasquez, C.M. Lennon, P.J. Smith, R.N. Jacobs, J.K. Markunas, L.A. Almeida, A. Stoltz, J.M. Arias, P.S. Wijewarnasuriya, J. Peterson, M. Reddy, M.F. Vilela, S.M. Johnson, D.D. Lofgreen, A. Yulius, M. Carmody, R. Hirsch, J. Fiala and S. Motakef , *J. Electron. Mater.* 44, 3082 (2015).
9. J.D. Benson, L.O. Bubulac, M. Jaime-Vasquez, C.M. Lennon, J.M. Arias, P.J. Smith, R.N. Jacobs, J.K. Markunas, L.A. Almeida, A. Stoltz, P.S. Wijewarnasuriya, J. Peterson, M. Reddy, K. Jones, S.M Johnson and D.D. Lofgreen, *J. Electron. Mater.* 45, 4052 (2016).
10. J.D. Benson, L.O. Bubulac, M. Jaime-Vasquez, J.M. Arias, P.J. Smith, R.N. Jacobs, J.K. Markunas, L.A. Almeida, A. Stoltz, P.S. Wijewarnasuriya, J. Peterson, M. Reddy, K. Jones, S.M Johnson and D.D. Lofgreen, *J. Electron. Mater.* 46, 5418 (2017).

Dette er en postprint-versjon/This is a postprint version.
DOI til publisert versjon/DOI to published version: 10.1007/s11664-019-07349-6

11. A. Noda, H. Kurita and R. Hirano, in Mercury Cadmium Telluride: Growth, Properties and Applications, ed. P. Capper and J. Garland (John Wiley & Sons, 2010), 21.

12. R.D.S. Yadava, B.S. Sundersheshu, M. Anandan, R.K. Bagai, and W.N. Borle, *J. Electron. Mater.* 23, 1349 (1994).

13. S. Sen, D.R. Rhiger, C.R. Curtis, M.H. Kalisher, H.L. Hettich, and M.C. Currie, *J. Electron. Mater.* 30, 611 (2001).

14. H. Bensalah, J. Crocco, V. Carcelén, A. Black, Q. Zheng, J.L. Plaza, and E. Diéguez, *J. Cryst. Growth* 361, 5 (2012).

15. L. Yujie, G. Zhi, L. Guoqiang and J. Wangqi, *J. Electron. Mater.* 33, 861 (2004).

16. E. Belas, M. Bugár, R. Grill, J. Franc, P. Moravec, P. Hlídec and P. Höschl, *J. Electron. Mater.* 37, 1212 (2008).

17. E. Selvig, K.O. Kongshaug, R. Haakenaasen, T. Lorentzen and T. Brudevoll, 'Transmission spectra of CdZnTe' *J. Electron. Mater.*same issue as this paper.

Dette er en postprint-versjon/This is a postprint version.
DOI til publisert versjon/DOI to published version: 10.1007/s11664-019-07349-6

FIGURE CAPTIONS

Fig. 1. (a) SEM image of the beveled edges at a corner of SubE, (b) a higher resolution image of the light-colored continuous layer of grit particles on the bevel edge, (c) a higher resolution image from the darker band on the bevel edge, and (d) EDS spectra from the plane surface away from the edge (grey), and from the beveled edge (black line).

Fig. 2. Images from SubA as-received: (a) dark field optical microscopy image of the surface, (b) SEM image of center of surface, (c) SEM image of some particles near the beveled edge, (d) higher resolution image of small silica grit particles in (c), (e) SEM image of larger CZT particle close to edge, and (f) AFM image near the middle of the substrate.

Fig. 3. (a) FTIR transmission spectra from an array of 11×11 points on SubA, and (b) map of the transmission values at 500 cm^{-1} from the spectra in (a).

Fig. 4. Images from SubA after surface preparation etching: (a) dark field optical microscopy image of surface near center, (b) SEM image of surface near an edge, (c) SEM image of particles near the beveled edge: flakes of silica grit particles (upper) and stains with Br, C and O (lower), (d) AFM image near the center, and (e) EDS spectrum from a 1270 x 890 um area near the center.

Fig. 5. SE and BSE images on SubA after etching: (a) a small agglomeration of silica grit particles and many Te precipitates, and (b) one grit particle and one Te precipitate.

Fig. 6. SE and BSE images of (a) a pattern of very small Te precipitates and (b) a similar pattern as in (a), but with a large Te precipitate in the middle. (c) EDS spectra from a Te precipitate (black line) and from area outside the precipitate (solid blue). The precipitate is shown in the inset.

Fig. 7. SE and BSE images of a Te precipitate from which a small piece has broken off and seems to have re-attached nearby. Insets are magnifications of the precipitate and the broken piece.

Dette er en postprint-versjon/This is a postprint version.
DOI til publisert versjon/DOI to published version: 10.1007/s11664-019-07349-6

Fig. 8. Images of SubB as-received, all near the center of the sample: (a) dark field image, (b) SEM image and (c) AFM image.

Fig. 9. Particles found on as-received SubB: (a) alumina and silica grit, (b) CdZnTe, (c) dark particles with size 20-30 μm containing a lot of carbon, (d) and (e) a stained area and particles with Na, Cl and O which could be NaClO, (f) an iron particle, (g) circular bright stains, (h) dark stains and (i) and (j) irregularly shaped voids of size 5-100 μm.

Fig. 10. FTIR transmission measurements recorded from an 11×11 grid on as-received SubB2: (a) Transmission spectra, (b) transmission map at wavenumber $k = 500\ \text{cm}^{-1}$. The spikes near $k = 4500\ \text{cm}^{-1}$ and $k = 5000\ \text{cm}^{-1}$ were artifacts of the FTIR instrument and should be ignored.

Fig. 11. Images from SubB/SubB2 after surface preparation etching: (a) dark field from SubB, (b) and (c) SEM images from SubB and SubB2, respectively, (d) alumina grit, (e) HgTe particle, (f) particle with carbon and fluorine, and (g) AFM image of SubB near the center.

Fig. 12. Images from SubC as -received: (a) dark field image, (b) SEM image near center with inserts of silica grit and carbon particles, and (c) AFM image from center.

Fig 13. FTIR transmission measurements recorded from a 5×5 grid on as-received SubC: (a) Transmission spectra, and (b) transmission map at wavenumber $k = 500\ \text{cm}^{-1}$. The spikes near $k = 4500\ \text{cm}^{-1}$ and $k = 4800\ \text{cm}^{-1}$ were artifacts of the FTIR instrument.

Fig. 14. Images from SubC after surface preparation etch: (a) dark field image, (b) SEM image near center with inserts of agglomeration silica grit, one flake of silica grit and a carbon particle, and (c) AFM image from center.

Fig. 15. SIMS profiles of (a) silicon, (b) aluminum, and (c) iron across the film/substrate interface in HgCdTe grown on CdZnTe. The interface of the different samples are at depth 13, 19, 21 and 28 μm, in all the three plots, and there are labels with arrows to the peaks on the top of the graph.

Dette er en postprint-versjon/This is a postprint version.
DOI til publisert versjon/DOI to published version: 10.1007/s11664-019-07349-6

Figure 1

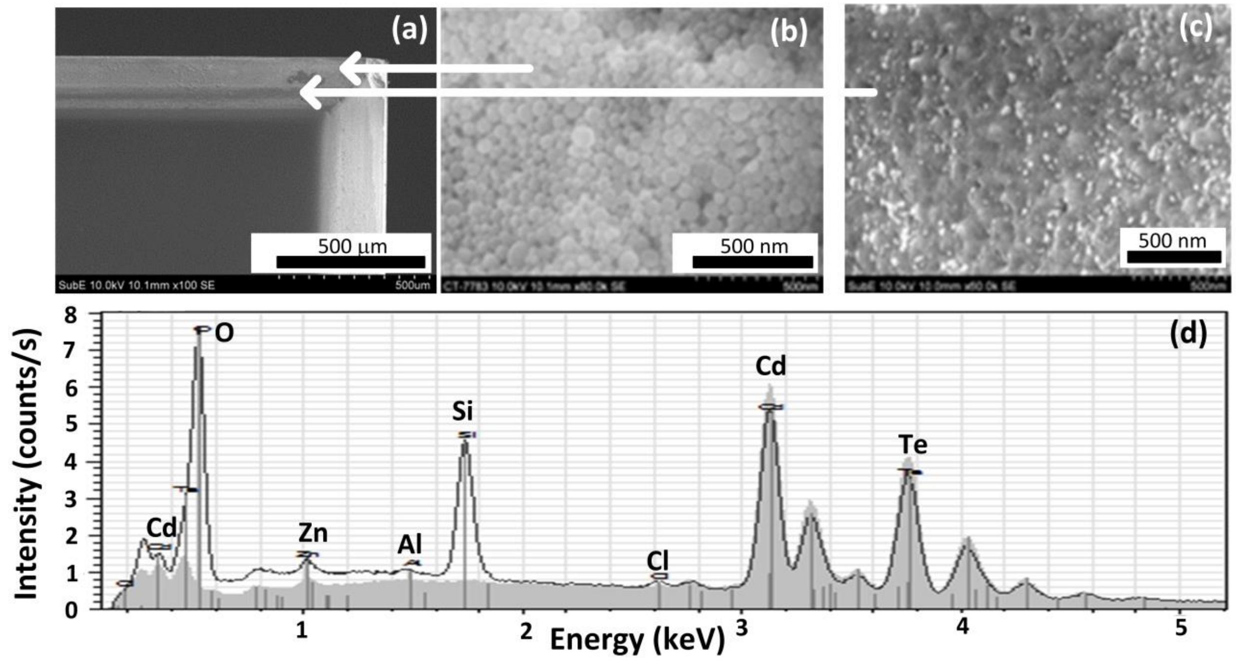

Figure 2

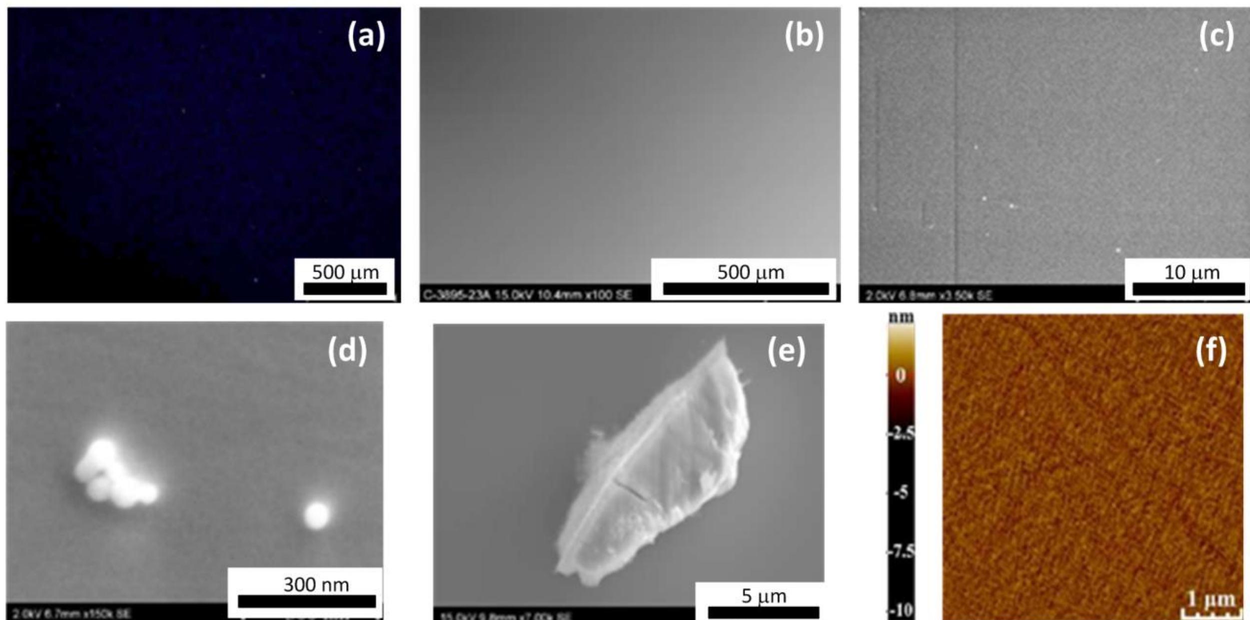

Dette er en postprint-versjon/This is a postprint version.
DOI til publisert versjon/DOI to published version: 10.1007/s11664-019-07349-6

Figure 3

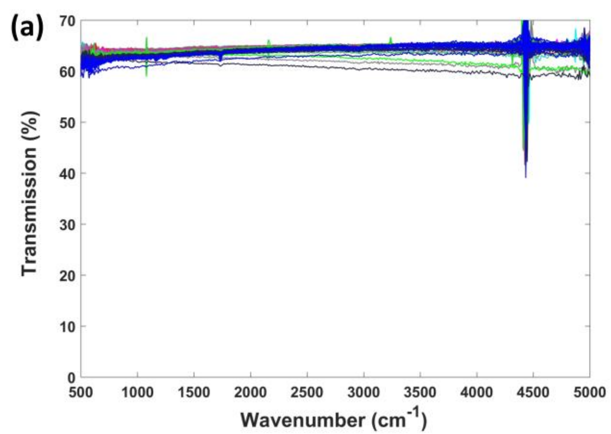

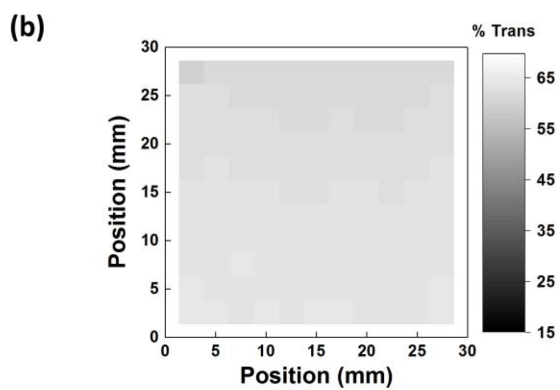

Dette er en postprint-versjon/This is a postprint version.
DOI til publisert versjon/DOI to published version: 10.1007/s11664-019-07349-6

Figure 4

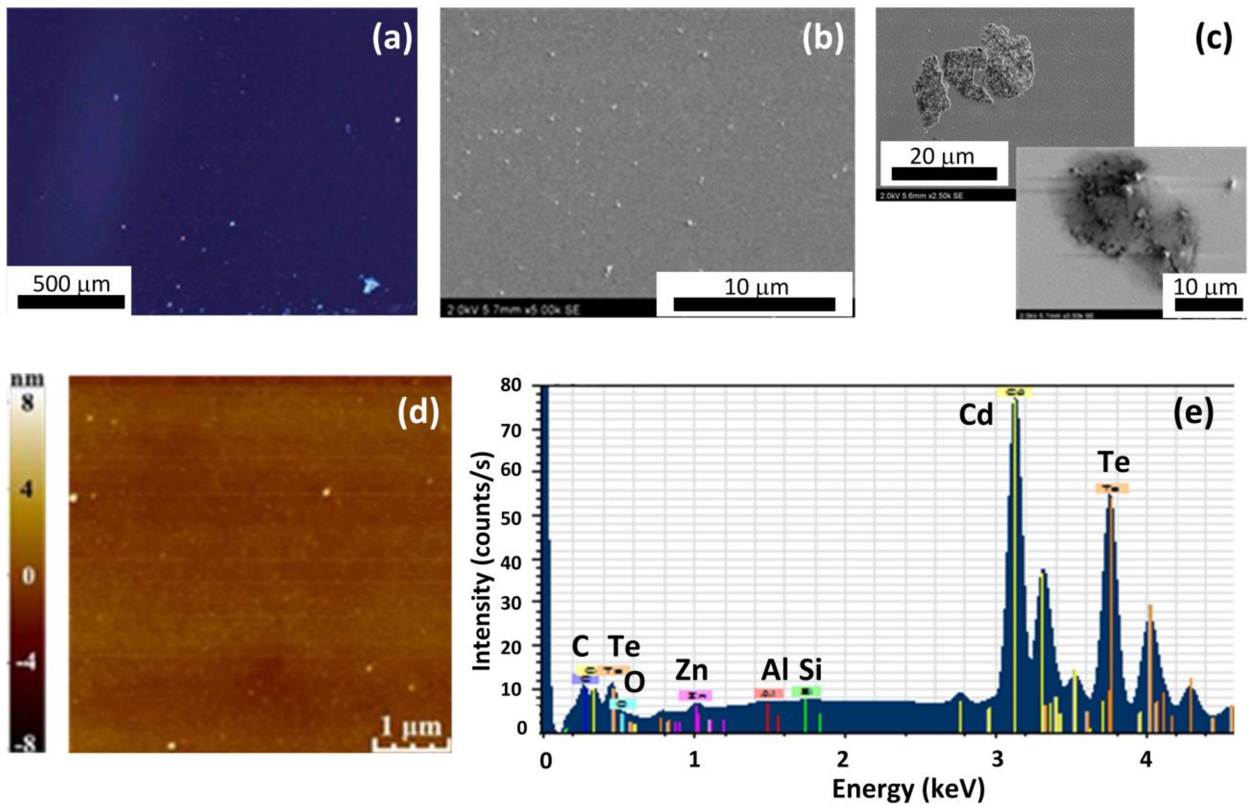

Figure 5

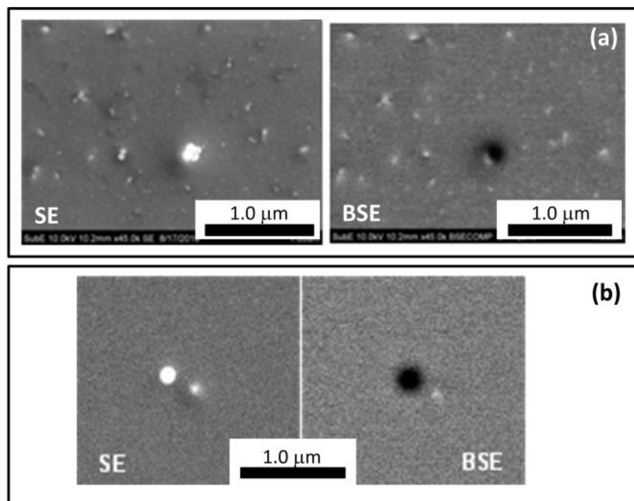

Dette er en postprint-versjon/This is a postprint version.
DOI til publisert versjon/DOI to published version: 10.1007/s11664-019-07349-6

Figure 6

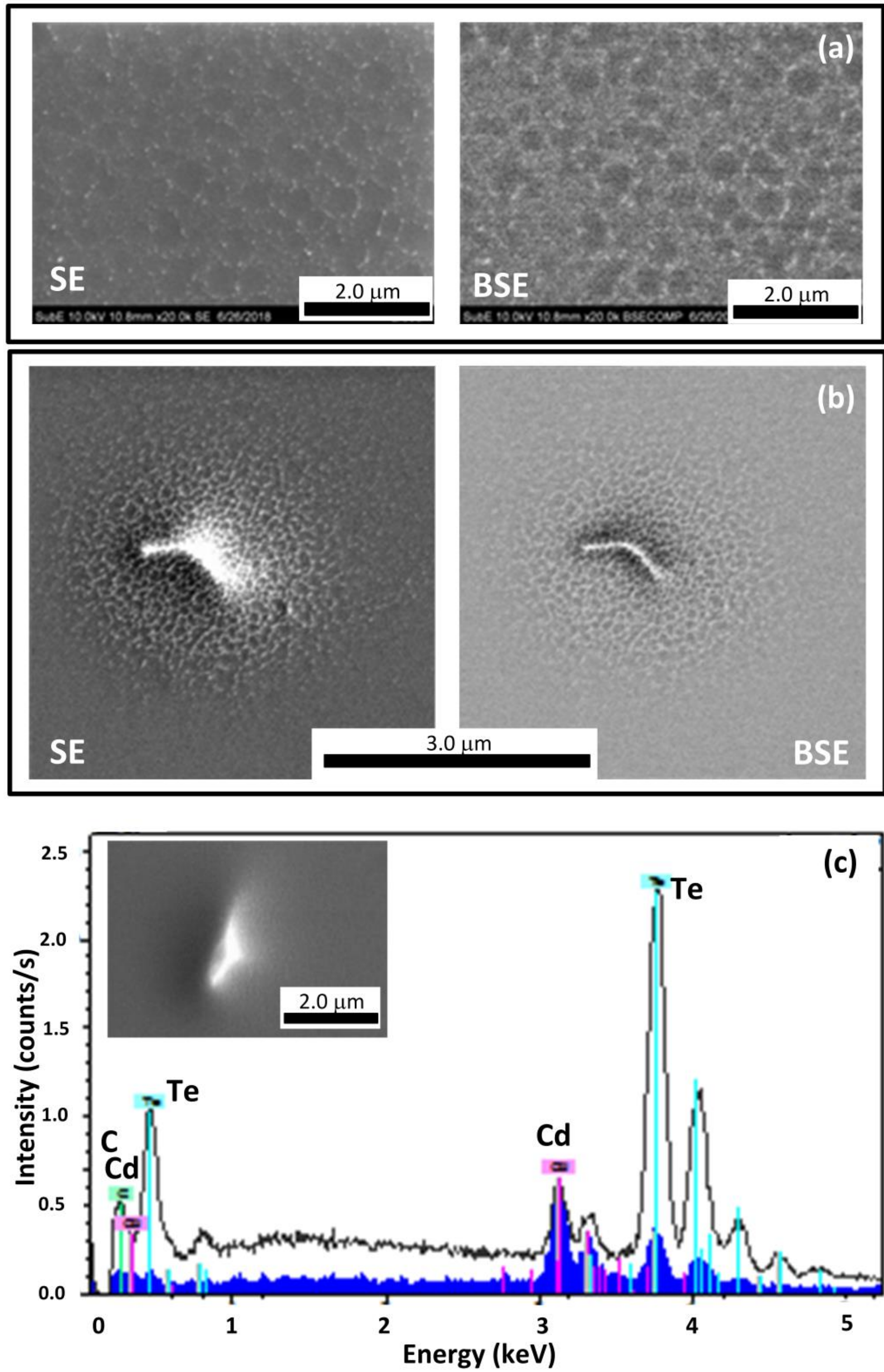

Dette er en postprint-versjon/This is a postprint version.
DOI til publisert versjon/DOI to published version: 10.1007/s11664-019-07349-6

Figure 7

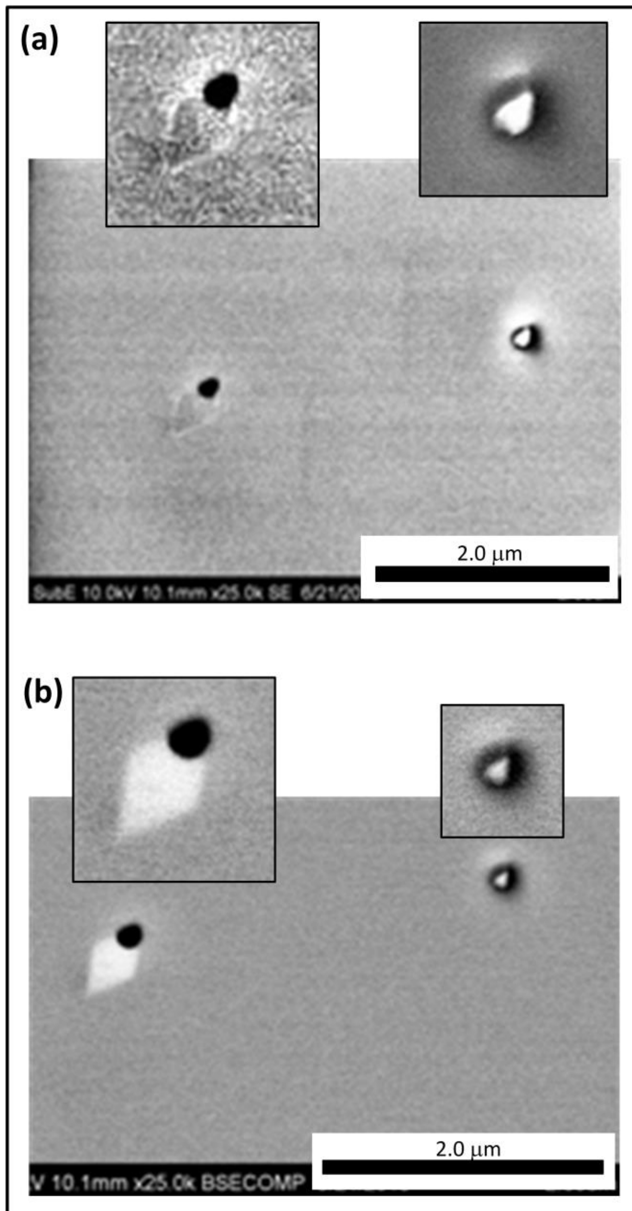

Dette er en postprint-versjon/This is a postprint version.
DOI til publisert versjon/DOI to published version: 10.1007/s11664-019-07349-6

Figure 8

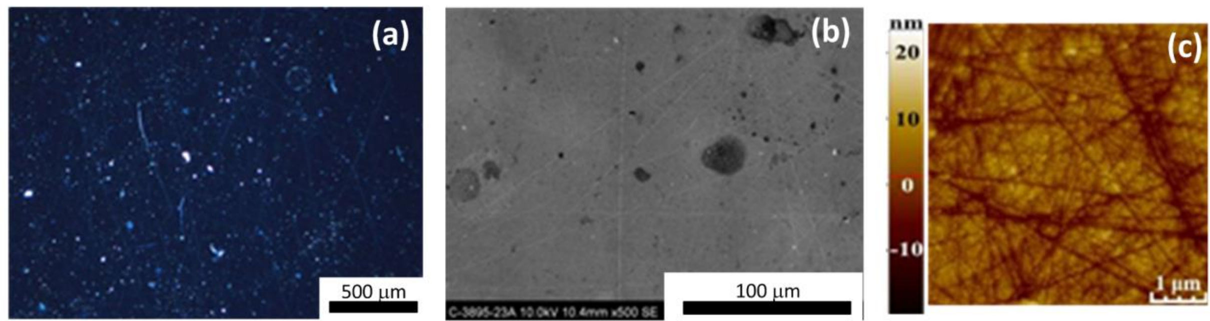

Figure 9

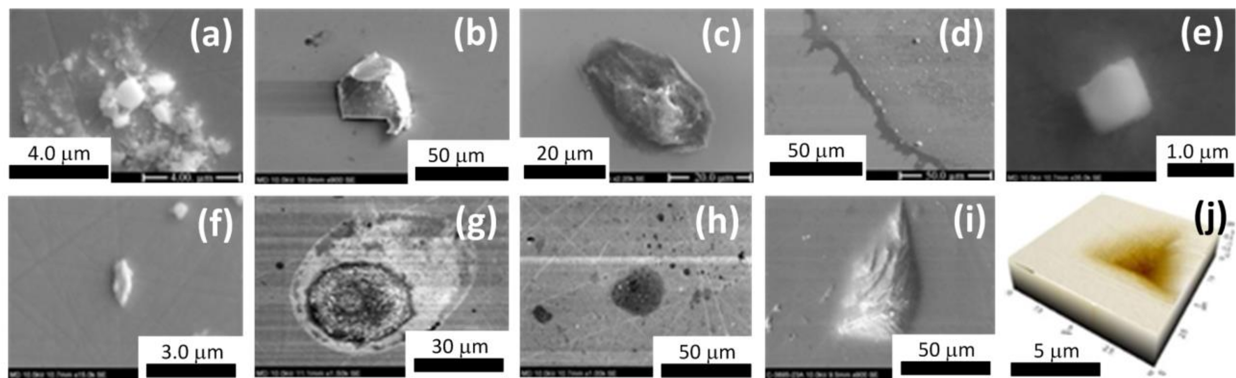

Dette er en postprint-versjon/This is a postprint version.
DOI til publisert versjon/DOI to published version: 10.1007/s11664-019-07349-6

Figure 10

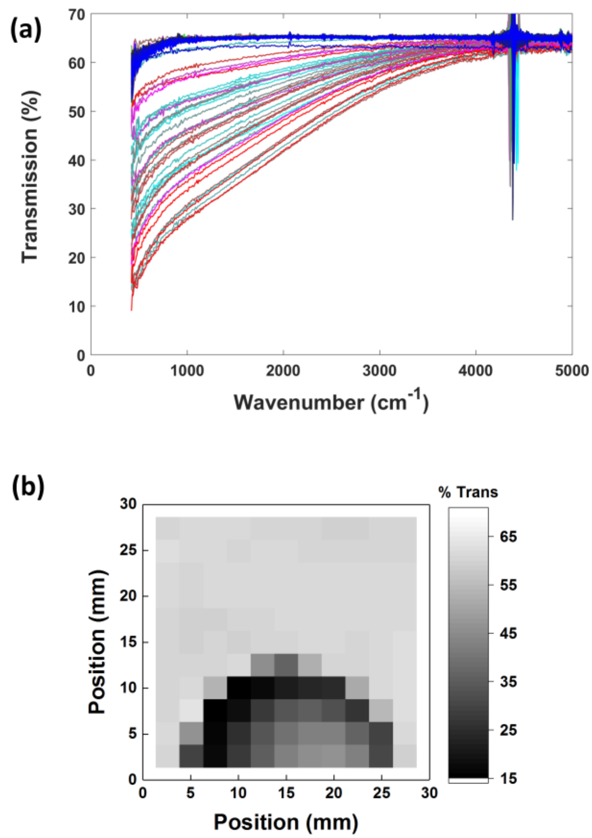

Figure 11

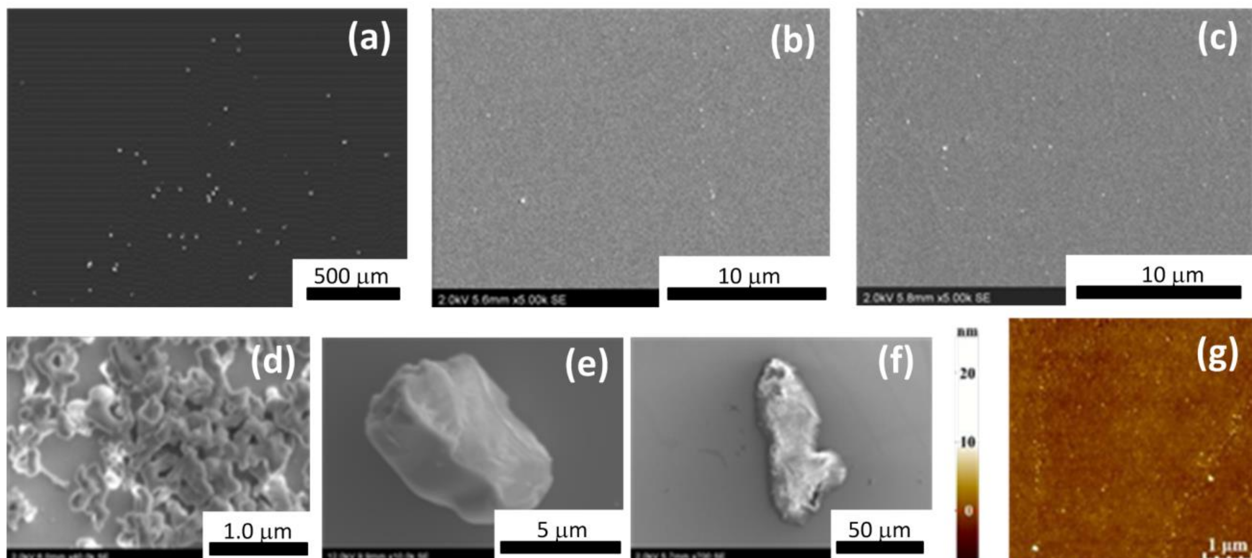

Dette er en postprint-versjon/This is a postprint version.
DOI til publisert versjon/DOI to published version: 10.1007/s11664-019-07349-6

Figure 12

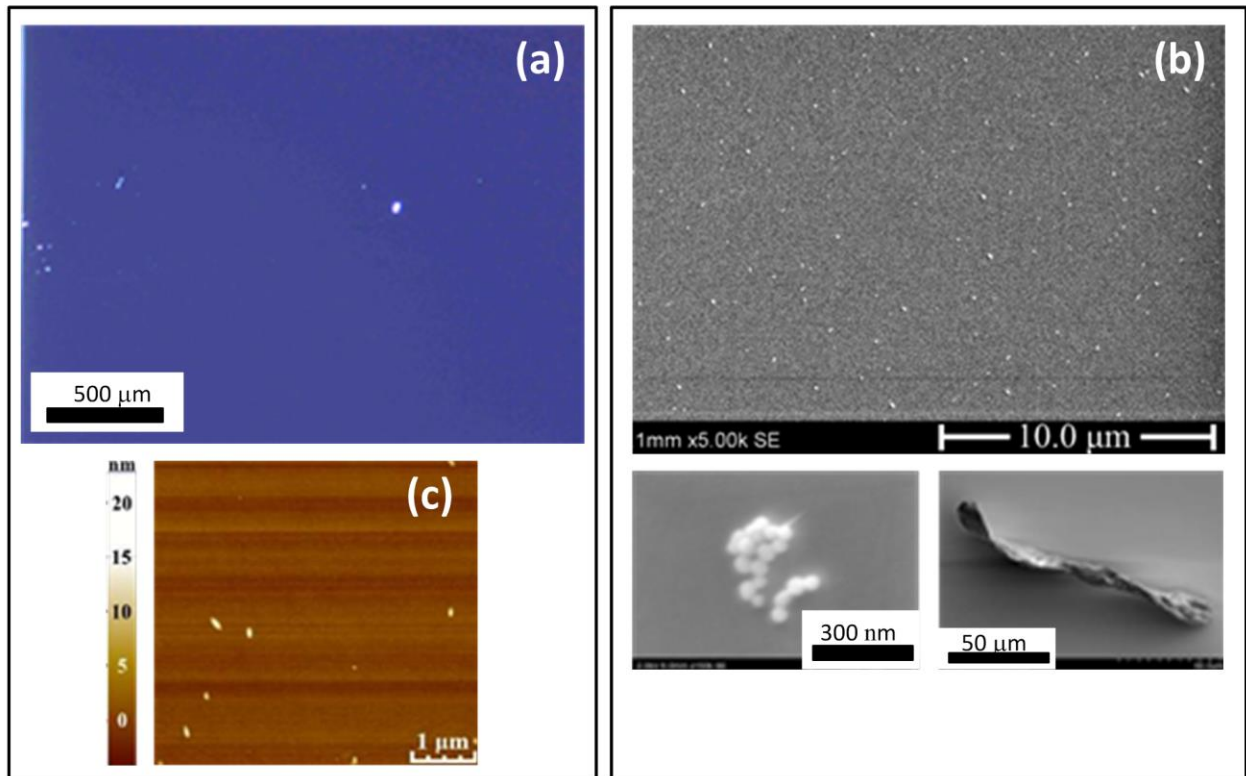

Figure 13

Dette er en postprint-versjon/This is a postprint version.
DOI til publisert versjon/DOI to published version: 10.1007/s11664-019-07349-6

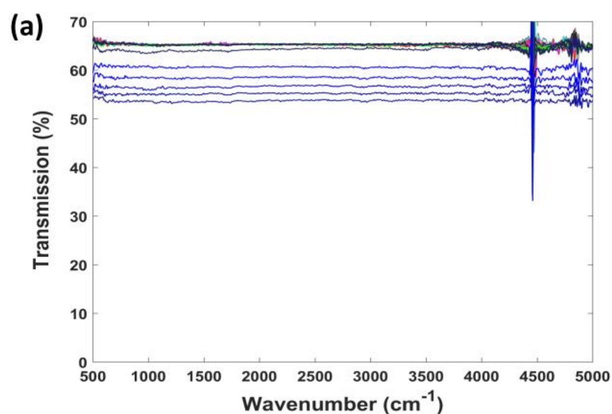

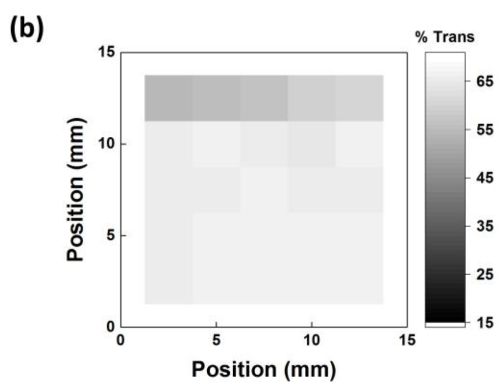

Figure 14

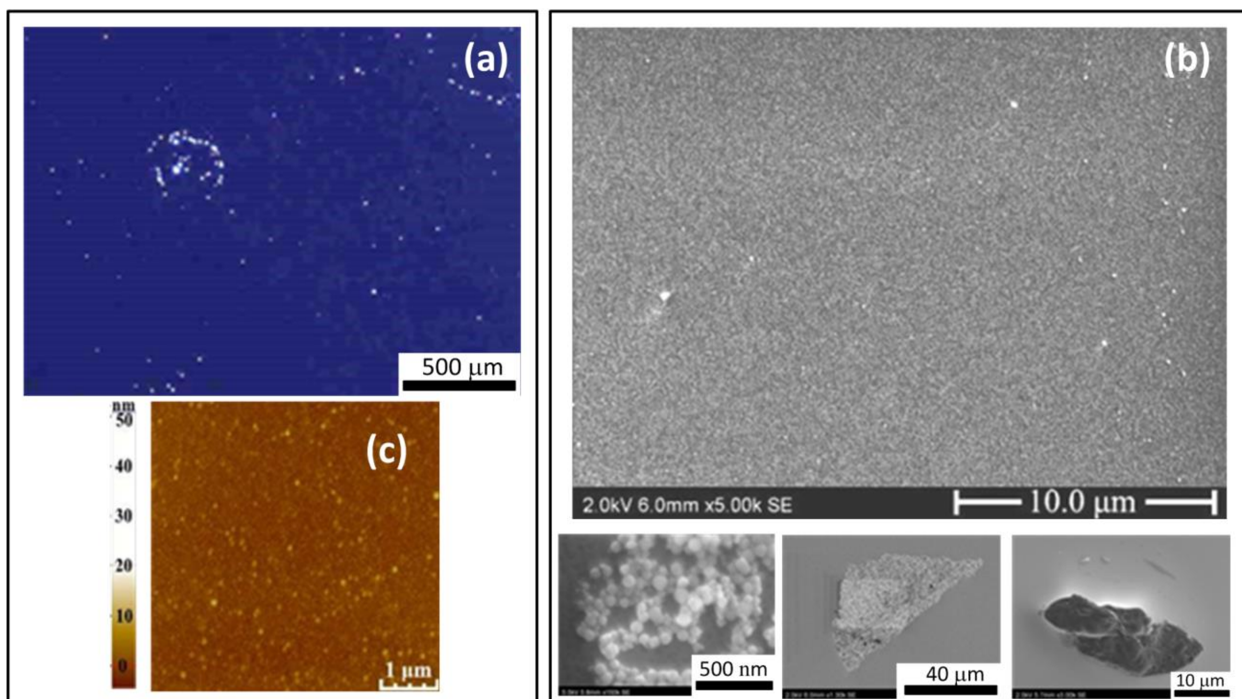

Dette er en postprint-versjon/This is a postprint version.
DOI til publisert versjon/DOI to published version: 10.1007/s11664-019-07349-6

Table I. Particle densities and AFM roughness before and after surface preparation

Substrate	Vendor	Orientation	Size (mm^2)	Large particles n_L (cm^{-2})	Te precipitates n_S (cm^{-2})	AFM roughness (nm)
SubA – as received	Nippon	(111)B	30 x 30	400	-	0.3
SubA – after surf. prep	Nippon	(111)B	30 x 30	1 000	2×10^6	0.5
SubB – as received	Alternative	(111)B	30 x 30	1×10^5	6×10^5	4
SubB – after surf. prep	Alternative	(111)B	30 x 30	5 000	7×10^6	0.85
SubB2-after surf.prep	Alternative	(111)B	30 x 30	5000	1×10^7	0.9
SubC – as received	Nippon	(211)B	15 x 15	30	3×10^7	0.95
SubC – after surf. prep	Nippon	(211)B	15 x 15	8 000	3×10^6	1.4

Dette er en postprint-versjon/This is a postprint version.
DOI til publisert versjon/DOI to published version: 10.1007/s11664-019-07349-6